The EMBO Journal (2013) 32, 1584–1597
www.embojournal.org

SOURCE DATA | TRANSPARENT PROCESS

THE EMBO JOURNAL

BRCA1 is a negative modulator of the PRC2 complex

Lan Wang[1,2,8], Xianzhuo Zeng[1,2,8], Shuai Chen[3,8], Liya Ding[1,2], Jian Zhong[1,2], Jonathan C Zhao[4], Liguo Wang[5], Aaron Sarver[3], Antonius Koller[6], Jizu Zhi[6], Yupo Ma[6], Jindan Yu[4], Junjie Chen[7] and Haojie Huang[1,2,*]

[1]Department of Biochemistry and Molecular Biology, Mayo Clinic College of Medicine, Rochester, MN, USA, [2]Mayo Clinic Cancer Center, Mayo Clinic College of Medicine, Rochester, MN, USA, [3]Masonic Cancer Center, University of Minnesota, Minneapolis, MN, USA, [4]Divison of Hematology/Oncology, Department of Medicine, Northwestern University Feinberg School of Medicine, Chicago, IL, USA, [5]Department of Biomedical Statistics and Informatics, Mayo Clinic College of Medicine, Rochester, MN, USA, [6]Department of Pathology, Stony Brook University Medical Center, Stony Brook, NY, USA and [7]Department of Experimental Radiation Oncology, University of Texas M. D. Anderson Cancer Center, Houston, TX, USA

The Polycomb-repressive complex 2 (PRC2) is important for maintenance of stem cell pluripotency and suppression of cell differentiation by promoting histone H3 lysine 27 trimethylation (H3K27me3) and transcriptional repression of differentiation genes. Here we show that the tumour-suppressor protein BRCA1 interacts with the Polycomb protein EZH2 in mouse embryonic stem (ES) and human breast cancer cells. The BRCA1-binding region in EZH2 overlaps with the noncoding RNA (ncRNA)-binding domain, and BRCA1 expression inhibits the binding of EZH2 to the HOTAIR ncRNA. Decreased expression of BRCA1 causes genome-wide EZH2 re-targeting and elevates H3K27me3 levels at PRC2 target loci in both mouse ES and human breast cancer cells. BRCA1 deficiency blocks ES cell differentiation and enhances breast cancer migration and invasion in an EZH2-dependent manner. These results reveal that BRCA1 is a key negative modulator of PRC2 and that loss of BRCA1 inhibits ES cell differentiation and enhances an aggressive breast cancer phenotype by affecting PRC2 function.

The EMBO Journal (2013) **32,** 1584–1597. doi:10.1038/emboj.2013.95; Published online 26 April 2013
Subject Categories: chromatin & transcription; molecular biology of disease
Keywords: BRCA1; breast cancer; embryonic stem cell; epigenetic gene silencing; PRC2

*Corresponding author. Department of Biochemistry and Molecular Biology, Mayo Clinic College of Medicine, Rochester, MN 55905, USA. Tel.: +1 507 293 1712; Fax: +1 507 293 3071; E-mail: huang.haojie@mayo.edu
[8]These authors contributed equally to this work

Received: 28 September 2012; accepted: 3 April 2013; published online: 26 April 2013

Introduction

The evolutionally conserved Polycomb group (PcG) proteins play pivotal roles in transcription repression by forming chromatin-modifying complexes termed Polycomb-repressive complexes (PRCs) such as PRC1 and PRC2 (Kennison, 1995; Schwartz and Pirrotta, 2007; Simon and Kingston, 2009; Margueron and Reinberg, 2011). PRC2 contains four core subunits of EZH2, SUZ12, EED and RbAp46/48 in humans or E(z), Su(z)12, esc and Nurf55 in *Drosophila*. EZH2 is an enzymatic subunit of PRC2 that contains a SET domain catalysing histone H3 lysine 27 trimethylation (H3K27me3; Cao *et al*, 2002; Czermin *et al*, 2002; Kuzmichev *et al*, 2002; Muller *et al*, 2002). This chromatin mark is commonly associated with silencing of differentiation genes and has key roles in developmental patterning in organisms ranging from plants and flies to humans. PRC2 is important for embryonic stem (ES) cell self-renewal, cell-fate decisions and generation of inducible pluripotent stem (iPS) cells (Boyer *et al*, 2006; Lee *et al*, 2006; Ezhkova *et al*, 2009; Onder *et al*, 2012). EZH2 is often overexpressed or mutated in human solid and hematologic tumours and has been implicated in cancer progression (Varambally *et al*, 2002; Bracken *et al*, 2003; Kleer *et al*, 2003; Morin *et al*, 2010).

Mounting evidence indicates that the potent function of EZH2 is tightly regulated in diverse biological contexts. EZH2 expression is regulated by RB/p130-E2F pathways, microRNA 101 and sex hormones (Bracken *et al*, 2003; Varambally *et al*, 2008; Bohrer *et al*, 2010). Noncoding RNAs (ncRNAs) such as *HOTAIR* and *XIST* bind to and facilitate PRC2 occupancy on chromatin (Rinn *et al*, 2007; Zhao *et al*, 2008; Gupta *et al*, 2010). The protein kinase AKT phosphorylates EZH2 at serine 21, which inhibits PRC2-mediated H3K27me3 and gene silencing but activates Polycomb-independent oncogenic functions of EZH2 (Cha *et al*, 2005; Xu *et al*, 2012). Cyclin-dependent kinase 1 (CDK1) and CDK2 phosphorylate EZH2 at threonine 350 (T350) and 487 (T487) residues and regulate PRC2 recruitment to its target loci (Chen *et al*, 2010; Kaneko *et al*, 2010; Wei *et al*, 2011). T350 phosphorylation also enhances EZH2 binding to *HOTAIR* and *XIST* ncRNAs and accelerates turnover of phosphorylated EZH2 (Kaneko *et al*, 2010; Wu and Zhang, 2011). Moreover, the *Jumonji* C-containing protein Jarid2 has been shown to interact with and regulate PRC2 enzymatic activity and target gene occupancy in ES cells (Peng *et al*, 2009; Shen *et al*, 2009; Landeira *et al*, 2010; Li *et al*, 2010; Pasini *et al*, 2010).

Breast cancer susceptibility gene 1 (*BRCA1*) was identified as a hereditary cancer susceptibility gene (Miki *et al*, 1994). Heterozygous germline mutations of *BRCA1* predispose women to breast and ovarian cancer with a lifetime risk up to 85% by age 70 years (King *et al*, 2003; Wooster and Weber, 2003). Strikingly, the majority of breast cancers arising in *BRCA1* mutation carriers are of the basal-like phenotype with unique characteristics such as lack of estrogen receptor (ER) but expression of basal or myoepithelial cell markers

cytokeratins (CKs) CK5/6, CK14 and CK17 (Foulkes *et al*, 2003; Sorlie *et al*, 2003; Foulkes, 2004; Lakhani *et al*, 2005). It has therefore been suggested that *BRCA1* tumours are originated from basal-like stem cells (Foulkes, 2004; Vassilopoulos *et al*, 2008). To date, a large number of biochemical activities have been linked to BRCA1 function, which include DNA damage response and repair (Scully *et al*, 1997; Cortez *et al*, 1999), transcription regulation (Chapman and Verma, 1996; Harkin *et al*, 1999), chromatin remodelling (Bochar *et al*, 2000), heterochromatin maintenance (Zhu *et al*, 2011), among others. Moreover, the NH2-terminal RING domain and the COOH-terminal BRCT domain have been identified as two major functional domains of BRCA1 (Huen *et al*, 2010). However, how BRCA1 regulates cell differentiation and how BRCA1 deregulation contributes to development of aggressive phenotypes of basal-like breast tumours remain elusive. In the present study we report that BRCA1 binds to EZH2 and modulates its functions in regulation of transcription repression, ES cell differentiation and breast cancer cell migration and invasion.

Results

BRCA1 associates with the PRC2 complex in ES and breast cancer cells

It has been shown previously that expression of PRC2 target genes are downregulated in ER-negative, basal-like breast cancers in comparison to other subtypes of breast cancer (Ben-Porath *et al*, 2008). Given that the vast majority of breast cancers arising from BRCA1 mutation carriers are of basal-like phenotype (Foulkes *et al*, 2003; Sorlie *et al*, 2003), we hypothesized that BRCA1 functions as a negative regulator of PRC2 and that loss of BRCA1 enhances PRC2 function. To test this hypothesis, we assessed whether BRCA1 protein interacts with PRC2. The 293T cells were transfected with myc-tagged EZH2 and cell lysates were subjected to co-immunoprecipitation (co-IP). As expected, the PRC2 core components SUZ12 and EED were detected in the anti-myc immunoprecipitants (Figure 1A). BRCA1 protein was also immunoprecipitated by anti-myc antibody, but not nonspecific IgG (Figure 1A). In contrast, BRCA1-associated RING domain protein 1 (BARD1) was not found in this complex (Figure 1A), suggesting a specific interaction between EZH2 and BRCA1. Neither BARD1 overexpression nor T350 phosphorylation on EZH2 affected the interaction (Supplementary Figure S1A and B). Next, we examined if endogenous BRCA1 interacts with PRC2. Ethidium bromide was added in co-IP assays to exclude DNA/chromatin as a potential mediator of protein interaction as reported previously (van der Vlag and Otte, 1999; Pasini *et al*, 2008). Endogenous BRCA1 protein along with endogenous PRC2 proteins Suz12 and Eed were immunoprecipitated by anti-Ezh2 from R1 mouse ES cells (Figure 1B). Reciprocally, endogenous PRC2 proteins Ezh2 and Suz12 were immunoprecipitated by anti-Brca1 antibody

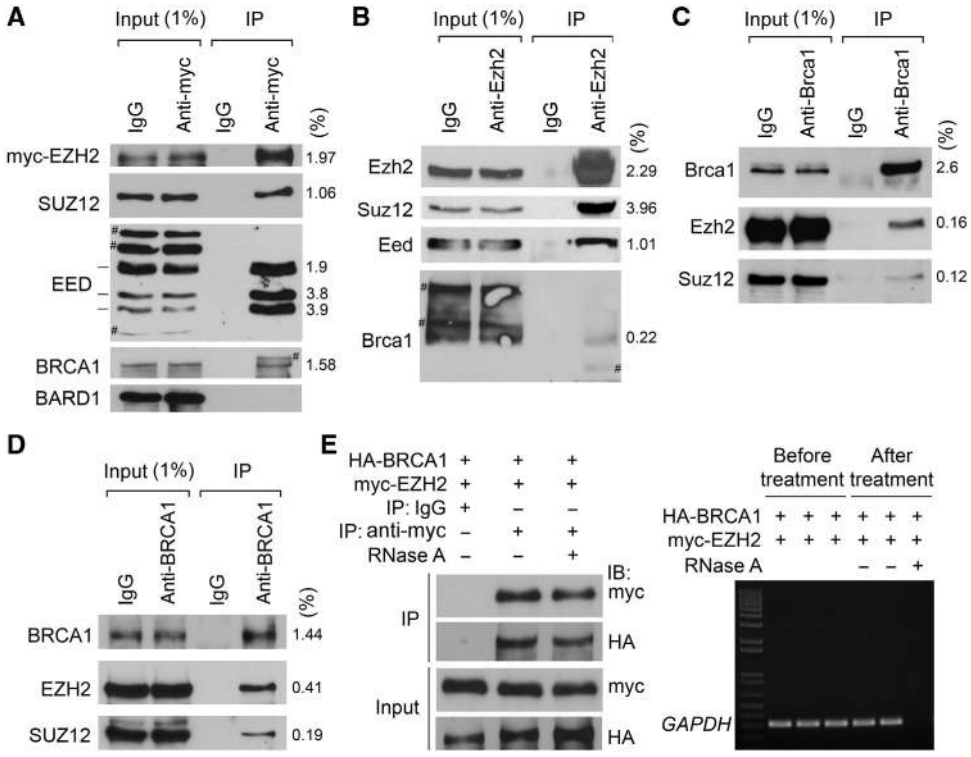

Figure 1 BRCA1 interacts with the PRC2 complex in ES and breast cancer cells. (**A**) Co-IP of myc–EZH2 with BRCA1 and PRC2 components SUZ12 and EED in 293T cells. The 293T cells transfected with myc-tagged EZH2 were subjected to Co-IP with anti-myc antibody. #Nonspecific proteins reacted with the antibodies used. The proportion (%) of each protein involved in the interaction is determined by dividing the immunoblotting band density of immunoprecipitant with the band density of input (1%), and shown in the right side of each blot. (**B**) Co-IP of endogenous Brca1 and PRC2 proteins by anti-Ezh2 antibody in R1 mouse ES cells. #Nonspecific proteins reacted with anti-BRCA1 antibody. (**C**) Co-IP of endogenous Ezh2, Suz12 and Brca1 proteins by anti-Brca1 antibody in AB2.2 mouse ES cells. (**D**) Co-IP of endogenous EZH2, SUZ12 and BRCA1 proteins by anti-BRCA1 antibody in MCF7 cells. (**E**) Effect of RNase A treatment on BRCA1–EZH2 interaction. The 293T cells transfected with HA–BRCA1 and myc–EZH2 and cell lysates were treated with or without RNase A prior to co-IP with anti-myc antibody (left) and RT–PCR for the presence of *GAPDH* mRNA. Source data for this figure is available on the online supplementary information page.

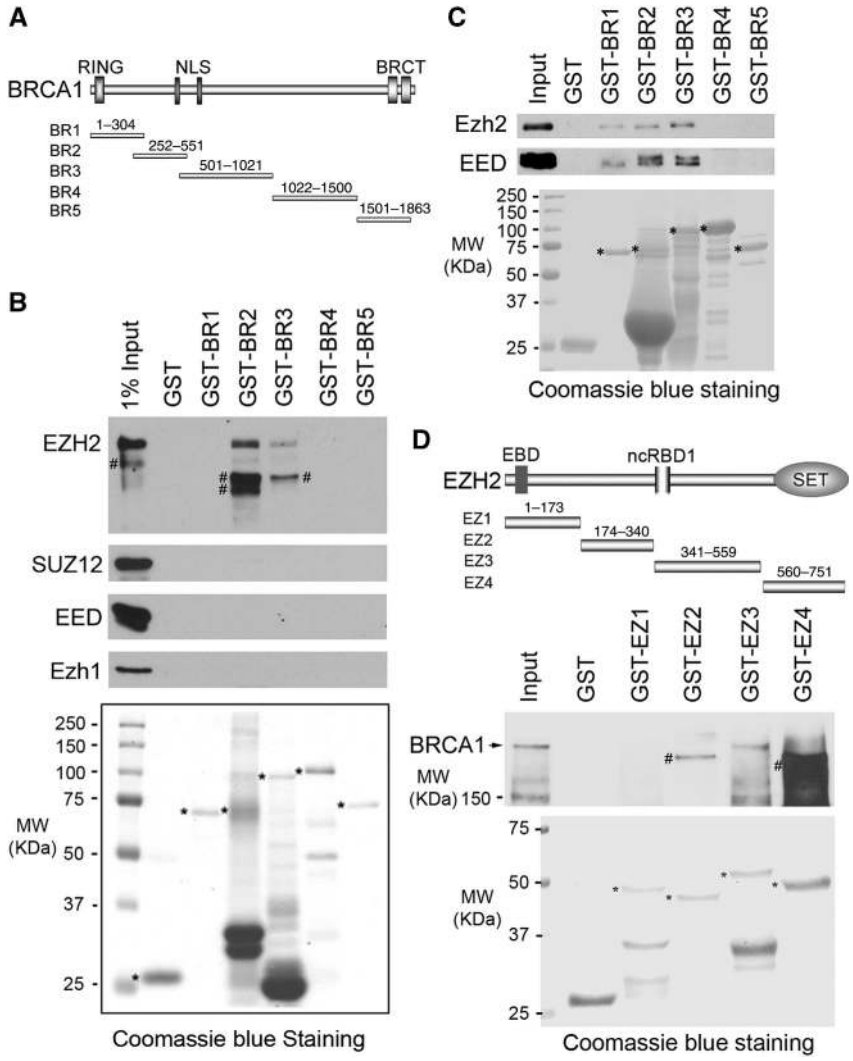

Figure 2 Analysis of the regions in BRCA1 and EZH2 responsible for their interaction. (**A**) Schematic diagram of the five GST-BRCA1 fusion proteins (BR1 to BR5). NLS, nuclear localization signal. (**B**) GST pull-down assay detecting the regions of BRCA1 that bind to PRC2 proteins. Top, western blot analysis of *in vitro* transcribed and translated Polycomb proteins EZH2, SUZ12, EED and Ezh1 pulled down by GST or GST-BRCA1 fusion proteins BR1-BR5. #Nonspecific proteins reacted with anti-EZH2 antibody. Bottom, Coomassie blue staining of GST and GST-BRCA1 fusion proteins BR1–BR5. Asterisks indicate proteins with correct molecular masses. (**C**) Top, western blot analysis of Ezh2 and EED in baculovirally expressed PRC2 complex pulled down by GST or GST-BRCA1 fusion proteins. Bottom, Coomassie blue staining of GST and GST-BRCA1 fusion proteins BR1–BR5. Asterisks indicate proteins with correct molecular masses. (**D**) GST pull-down assay detecting the regions of EZH2 that bind to BRCA1. Top, schematic diagram of the four GST-EZH2 fusion proteins designated as EZ1 to EZ4. EBD, EED binding domain; ncRBD1, ncRNA binding domain 1. Middle, western blot analysis of baculovirally expressed BRCA1 pulled down by GST or GST-EZH2 fusion proteins EZ1-EZ4. #Nonspecific proteins reacted with anti-BRCA1 antibody. Bottom, Coomassie blue staining of GST and GST-EZH2 fusion proteins EZ1–EZ4. Asterisks indicate proteins with correct molecular mass. Source data for this figure is available on the online supplementary information page.

from AB2.2 mouse ES cells (Figure 1C). Parallel interactions were detected in human breast cancer cell line MCF7 (Figure 1D). Together, both endogenous and ectopically expressed BRCA1 and EZH2 interact with each other in various cell types.

Identification of region(s) in BRCA1 and EZH2 responsible for their interaction

We performed glutathione *S*-transferase (GST) pull-down assays to determine if BRCA1 directly interacts with EZH2 and which region(s) in BRCA1 and EZH2 proteins mediates their interaction. EZH2, SUZ12, EED and Ezh1 were produced individually by *in vitro* transcription and translation and incubated separately with bacteria-purified five GST-BRCA1 fusion proteins (Figure 2A). Only EZH2, but not SUZ12, EED and Ezh1 interacted with BRCA1, although similar amounts of proteins were used (Figure 2B). There were two regions in BRCA1 (BR2, amino acids 252–551 and BR3, amino acids 501–1021) that interacted with EZH2 (Figure 2B). When the recombinant PRC2 complex containing Ezh2, SUZ12, EED and RbAp48 copurified from insect Sf9 cells was employed in GST pull-down assay, we found that the most NH2-terminal region in BRCA1 (BR1, amino acids 1–304) also interacted with EZH2 and EED in the PRC2 complex (Figure 2C), indicating that other subunits of PRC2 contribute to the interaction of BRCA1 with EZH2. The interaction between BRCA1 NH2-terminus and EZH2 was confirmed by co-IP and mass spectrometry analyses (Supplementary Figure S1C–F).

Reciprocally, recombinant BRCA1 proteins purified from Sf9 cells were incubated with GST-EZH2 fusion proteins. As shown in Figure 2D, BRCA1 interacted with a region in EZH2 containing amino acids 341–559, which overlaps with the ncRNA binding domain 1 (ncRBD1, amino acids 342–370) (Kaneko *et al*, 2010). Because the EZH2 interaction region in BRCA1 contains a RING domain and a similar domain in other proteins enables to bind to RNA (Lai *et al*, 1998), we sought to determine if the BRCA1–EZH2 interaction is RNA mediated. Cell lysates were treated with RNase A prior to co-IP. The effectiveness of RNase A treatment was evident by complete depletion of *GAPDH* mRNA from the cell lysates (Figure 1E, right). However, RNase A treatment had little or no effect on the BRCA1–EZH2 interaction (Figure 1E, left), suggesting that their interaction is not RNA mediated.

BRCA1 regulates genome-wide occupancy of EZH2 on chromatin

The interaction between BRCA1 and EZH2 prompted us to determine if BRCA1 affects EZH2 occupancy on its target genes. We employed a chromatin immunoprecipitation coupled with DNA microarray (ChIP-chip) approach to interrogate genome-wide chromatin occupancy of EZH2 in two independent mouse ES cell lines. Consistent with the previous report (Chang *et al*, 2009), Brca1 protein levels were significantly reduced in *Brca1*-heterozygous PL2F8 cells in comparison to wild-type AB2.2 ES cells, but was restored in PL2F8-BAC cells rescued with human BRCA1 BAC DNA (Figure 3A and Supplementary Figure S2A). Brca1-heterozygous deletion resulted in gain of Ezh2 occupancy on 1330 *de novo* targets (Figure 3B and Supplementary Table S1) and the result was reproducible (Supplementary Figure S2B). Brca1-heterozygous deletion also caused loss of Ezh2 occupancy on 646 pre-existing targets (Figure 3B). These results were unlikely caused by the effect of BRCA1 on cell proliferation since little or no difference in cell cycle distribution was observed between AB2.2 and PL2F8 cells (Supplementary Figure S2C). Similarly, Brca1 knockdown by small interference RNA (siRNA) in R1 mouse ES cells (Supplementary Figure S2D) induced gain of Ezh2 occupancy on 1081 *de novo* targets but loss of occupancy on 858 targets (net gain of 223 targets; Figure 3B and Supplementary Table S1). The overlap (218 genes) of the gained Ezh2 targets between PL2F8 and R1 siBr cells was relatively small, but reproducible and statistically significant (Figure 3B and C and Supplementary Figure S2E). This is probably due to a large degree of genetic diversity among 129 substrains (Simpson *et al*, 1997; Threadgill *et al*, 1997) from which AB2.2 and R1 ESC lines were established and the overt differences in Brca1 protein level in these two ESC lines both before and after Brca1 knockdown or knockout (Supplementary Figure S2F). It is worth noting that overexpression *HOTAIR* ncRNA also resulted in a biphasic effect on EZH2 targeting in breast cancer cells (Gupta *et al*, 2010). Gene ontology (GO) analysis of the 218 *de novo* Ezh2 targets showed that these genes are enriched for diverse functions including development, cell growth and adhesion (Supplementary Figure S3A). Additionally, *Brca1*-heterozygous deletion in PL2F8 cells enhanced Ezh2 occupancy on 1089 pre-existing PRC2 targets including *Hoxa9* (Figure 3D and Supplementary Table S1). Similarly, silencing of Brca1 in R1 cells also increased Ezh2 occupancy on a large number of pre-existing PRC2 targets (Supplementary Table S1). Brca1 deficiency-enhanced chromatin enrichment of Ezh2 in PL2F8 ES cells was confirmed by ChIP–qPCR at the promoters of 7 *de novo* and 3 pre-existing target genes including development regulators and tumour growth and metastasis suppressor genes *Brachyury* (*T*), *Dab2ip*, *Igfbp3*, *Adrb1* and *Adam10* (Peng *et al*, 2009; Xie *et al*, 2010) (Figure 3E). Restored BRCA1 expression in PL2F8-BAC cells reversed Ezh2 occupancy at these loci (Figure 3A and E). Collectively, these data indicate that reduced expression of BRCA1 broadens genome-wide occupancy of EZH2 on chromatin in murine ES cells.

BRCA1 regulates H3K27me3 levels at EZH2 target loci

Next, we sought to determine if BRCA1 affects H3K27me3 levels at EZH2 target loci. *Brca1*-heterozygous deletion had no effect on the level of PRC2 proteins Ezh2, Suz12 and Eed in PL2F8 cells compared to AB2.2 cells (Figure 3A), while it resulted in a substantial increase in H3K27me3 in the promoters of *de novo* and pre-existing PRC2 targets examined (Figure 3F). This effect was completely reversed by restored expression of BRCA1 in PL2F8-BAC ES cells (Figure 3F). To determine whether BRCA1 regulates PRC2 function in human breast cancer cells, endogenous BRCA1 was knocked down by two independent BRCA1-specific siRNAs in MCF7 cells (Figure 4A). Silencing of BRCA1 resulted in a significant increase in EZH2 occupancy and H3K27me3 levels in the promoter of *HOXA9* (Figure 4B, left). Accordingly, overexpression of BRCA1 decreased the binding of EZH2 to the *HOXA9* promoter and increased *HOXA9* mRNA expression (Figure 4C and D). Consistent with the findings that *Dab2ip* is not a PRC2 target in wild-type mouse ES cells (Ku *et al*, 2008), and that it is highly bound by Ezh2 due to heterozygous deletion of *Brca1* in PL2F8 ES cells (Figure 3D–F), EZH2 binding and H3K27me3 levels significantly increased at the *DAB2IP* locus in BRCA1-knockdown MCF7 cells (Figure 4B, right). BRCA1 knockdown also increased EZH2 occupancy and H3K27me3 levels in the promoter of *HOXA9* in MCF10A cells and other four EZH2 target loci in MCF7 cells (Figure 4E and Supplementary Figure S3B). Consistent with these observations, BRCA1 knockdown decreased the expression of HOXA9, DAB2IP and FOXJ1 proteins in MCF7 cells (Figure 4A). Thus, BRCA1 negatively regulates PRC2 function and loss of BRCA1 increases H3K27me3 levels at PRC2 target loci in both mouse ES and human breast cancer cells.

BRCA1 inhibits HOTAIR-enhanced EZH2 recruitment to its target loci

Since BRCA1 inhibits EZH2 occupancy on chromatin (Figure 3E and 4B) without affecting PRC2 component expression (Figure 3A), we sought to determine if BRCA1 influences PRC2 recruitment to its target loci. Several transcription regulators (e.g., YY1) and long ncRNAs (such as *HOTAIR* and *XIST*) have been shown to interact with and facilitate PRC2 targeting in mammalian cells (Caretti *et al*, 2004; Rinn *et al*, 2007; Zhao *et al*, 2008). Because the binding region of BRCA1 in EZH2 (amino acids 341–559) overlaps with the ncRBD1 (amino acids 342–370) (Kaneko *et al*, 2010), we examined if BRCA1 interferes EZH2 binding to ncRNAs. RNA immunoprecipitation (RIP) assay showed that expression of BRCA1 inhibited and BRCA1 knockdown

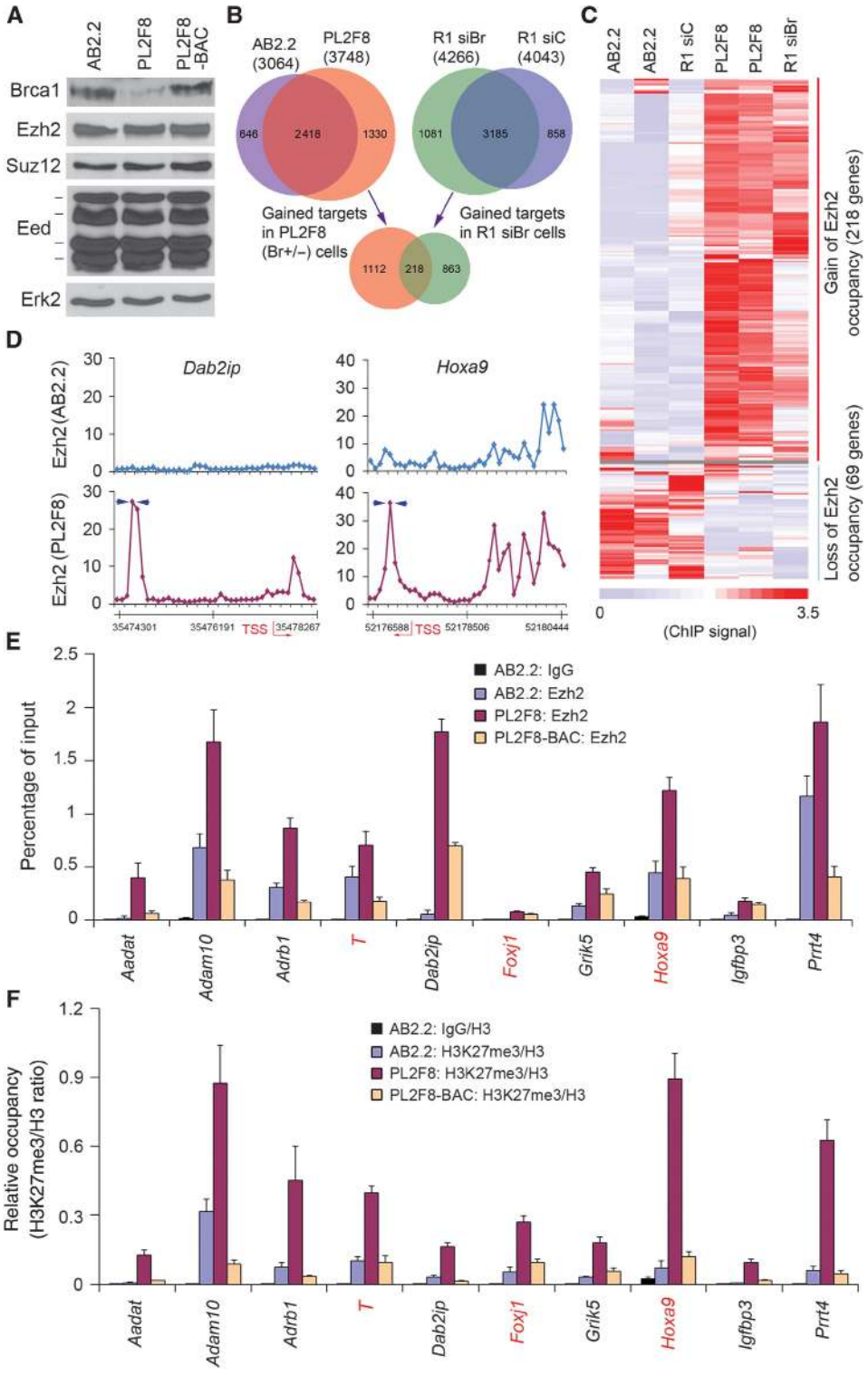

Figure 3 Effect of Brca1 expression on genome-wide Ezh2 targeting in mouse ES cells. (**A**) Western blot analysis of expression of indicated proteins in AB2.2, PL2F8 and PL2F8-BAC mouse ES clones. Expression of extracellular signal-regulated kinase 2 (Erk2) was included as a loading control. Data shown are from one representative experiment out of two independent experiments that gave similar results. (**B**) Venn diagram showing *de novo* Ezh2 targeting genes shared between PL2F8 cells with *Brca1* heterozygous deletion and R1 mouse ES cells with *Brca1* knockdown. The overlap is statistically significant with $P = 8.59E{-}31$ (hypergeometric test). (**C**) Heat map showing genes with gain or loss of Ezh2 occupancy due to decreased expression of Brca1 in three Brca1-proficient replicates (two AB2.2 plus one R1 siC) and three Brca1-deficient replicates (two PL2F8 plus one R1 siBr). ChIP signals are depicted using the colour scale at the bottom. (**D**) Examples of Ezh2 ChIP-chip results for the indicated loci in AB2.2 and PL2F8 ES cells. TSS, transcription start site. Arrows in blue indicate the locations of primers for ChIP–qPCR. (**E**) ChIP–qPCR analysis of Ezh2 occupancy on target loci in AB2.2, PL2F8 and PL2F8-BAC ES cells. Data are shown as means ± s.d. from experiments with three replicates ($n = 3$). Genes labelled in red are known EZH2 targets in mouse ES cells. (**F**) ChIP–qPCR analysis of H3K27me3 in PRC2 target loci identified by ChIP-chip in AB2.2, PL2F8 and PL2F8-BAC ES cells. Data are means ± s.d. from three individual experiments ($n = 3$). H3K27me3 and total H3 ChIP results were first normalized to input DNA and the H3K27me3/H3 ratio was determined by their normalized values. Genes labelled in red are known EZH2 targets. Source data for this figure is available on the online supplementary information page.

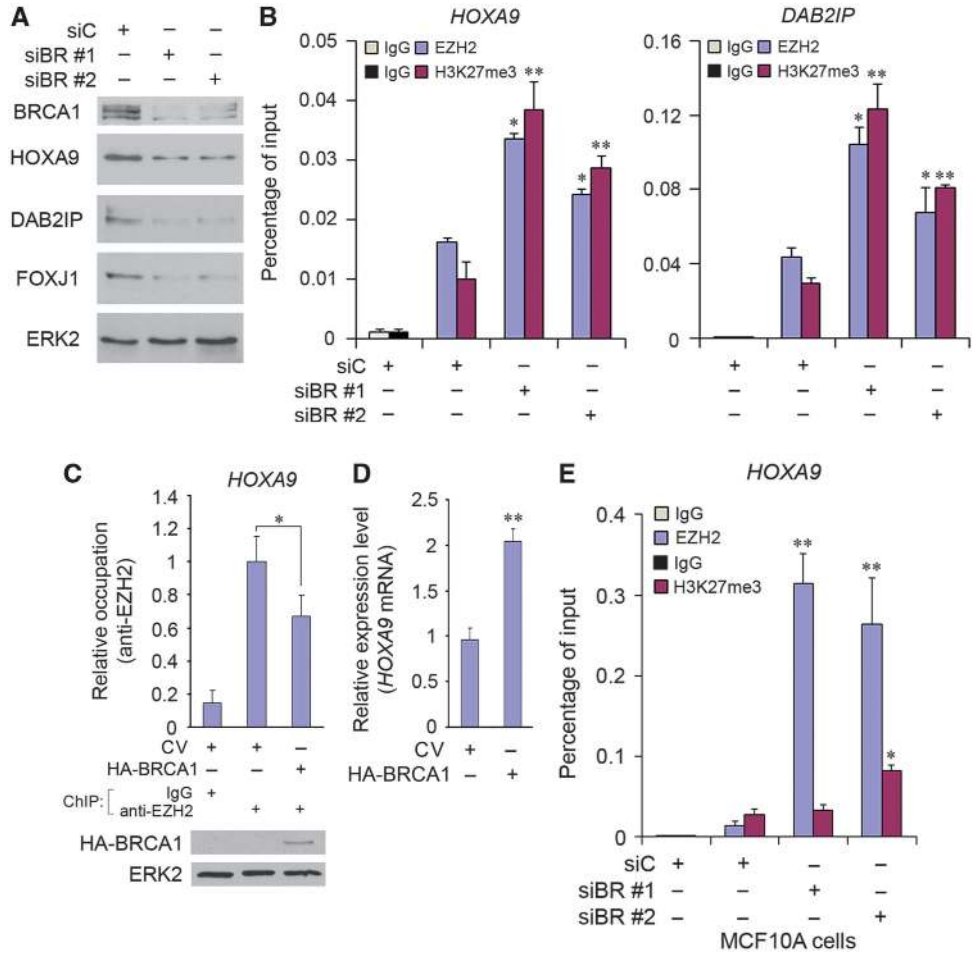

Figure 4 BRCA1 negatively regulates EZH2 recruitment and H3K27me3 levels at PRC2 target loci in breast cancer cells. (**A**) Western blot analysis of expression of BRCA1 and PRC2 target proteins HOXA9, DAB2IP and FOXJ1 in MCF7 cells transfected with control (siC) or two independent BRCA1-specific siRNAs. ERK2, loading control. (**B**) MCF7 cells were transfected with control and BRCA1-specific siRNAs as in (**A**) and subjected to ChIP analysis with anti-EZH2, anti-H3K27me3 antibodies or control IgG and qPCR analysis (means ± s.d., $n=3$). $^{*}P<0.05$ comparing EZH2 enrichment in siBR#1 and #2 transfected cells to that in siC transfected cells; $^{**}P<0.01$ comparing H3K27me3 enrichment in siBR#1 and #2 transfected cells to that in siC transfected cells. (**C**, **D**) Effects of BRCA1 overexpression on EZH2 recruitment to the *HOXA9* gene promoter and *HOXA9* mRNA expression in MCF7 cells. At 24 h after transfection, cells were subjected to western blot, ChIP–qPCR (means ± s.d., $n=3$) (**C**) and RT–qPCR (means ± s.d., $n=3$) (**D**). CV, control vector; $^{*}P<0.05$ and $^{**}P<0.01$. (**E**) ChIP–qPCR analysis of EZH2 and H3K27me3 enrichment on *HOXA9* gene promoter in MCF10A cells (means ± s.d., $n=3$). $^{**}P<0.01$ comparing EZH2 enrichment in siBR#1 and #2 transfected cells to that in siC transfected cells; $^{*}P<0.05$ comparing H3K27me3 enrichment in siBR#2 transfected cells to that in siC transfected cells. Source data for this figure is available on the online supplementary information page.

increased EZH2 binding to *HOTAIR* in MCF7 cells (Figure 5A and B). Consistent with the finding that *HOTAIR* is important for PRC2 targeting (Rinn *et al*, 2007; Kaneko *et al*, 2010), expression of *HOTAIR* increased the binding of EZH2 to the *HOXA9* promoter in MDA-MB-231 cells, but this effect was blocked by forced expression of BRCA1 (Figure 5C, left). BRCA1 also inhibited *HOTAIR*-enhanced EZH2 occupancy on *HOXA9* promoter in MCF7 cells and BJ human fibroblasts (Figure 5D). However, BRCA1 expression failed to inhibit EZH2 occupancy on EZH2 target loci in *HOTAIR*-knockdown MCF7 cells (Supplementary Figure S4A–C), suggesting that BRCA1-mediated inhibition of EZH2 occupancy on chromatin is mainly mediated through *HOTAIR* in MCF7 cells. Moreover, the *HOXA9* mRNA level was repressed by *HOTAIR* expression in MDA-MB-231 cells and this was completely reversed by forced expression of BRCA1 (Figure 5C, right). Thus, BRCA1 inhibits the binding of *HOTAIR* to EZH2 and abolishes *HOTAIR*-enhanced recruitment of PRC2 to its target gene *HOXA9* in human breast cancer cells and fibroblasts.

BRCA1 is involved in G2/M cell cycle checkpoint control. As expected, expression of wild-type BRCA1 in MDA-MB-231 cells increased cell cycle distribution at G2/M (Supplementary Figure S5A and B). In contrast, expression of BRCA1-N (amino acids 1–1100), a COOH-terminal truncation mutant of BRCA1, had no effect on G2/M distribution (Supplementary Figure S5A and B). This result is consistent with a previous report that stable expression of a COOH-terminal deletion mutant of BRCA1 had little or no effect on cell growth (Harkin *et al*, 1999). In agreement with the finding that BRCA1-N interacts with EZH2 *in vitro* and in cells (Figure 2C and Supplementary Figure S1C), ectopic expression of BRCA1-N not only inhibited EZH2 occupancy on chromatin at its target loci, but also increased its target gene expression (Supplementary

Figure S5C and D). Importantly, these effects of BRCA1-N were similar to those mediated by wild-type BRCA1 (Supplementary Figure S5C and D). Together, these data rule out the possibility that the effects of BRCA1 on EZH2 chromatin occupancy are due to cell cycle alterations.

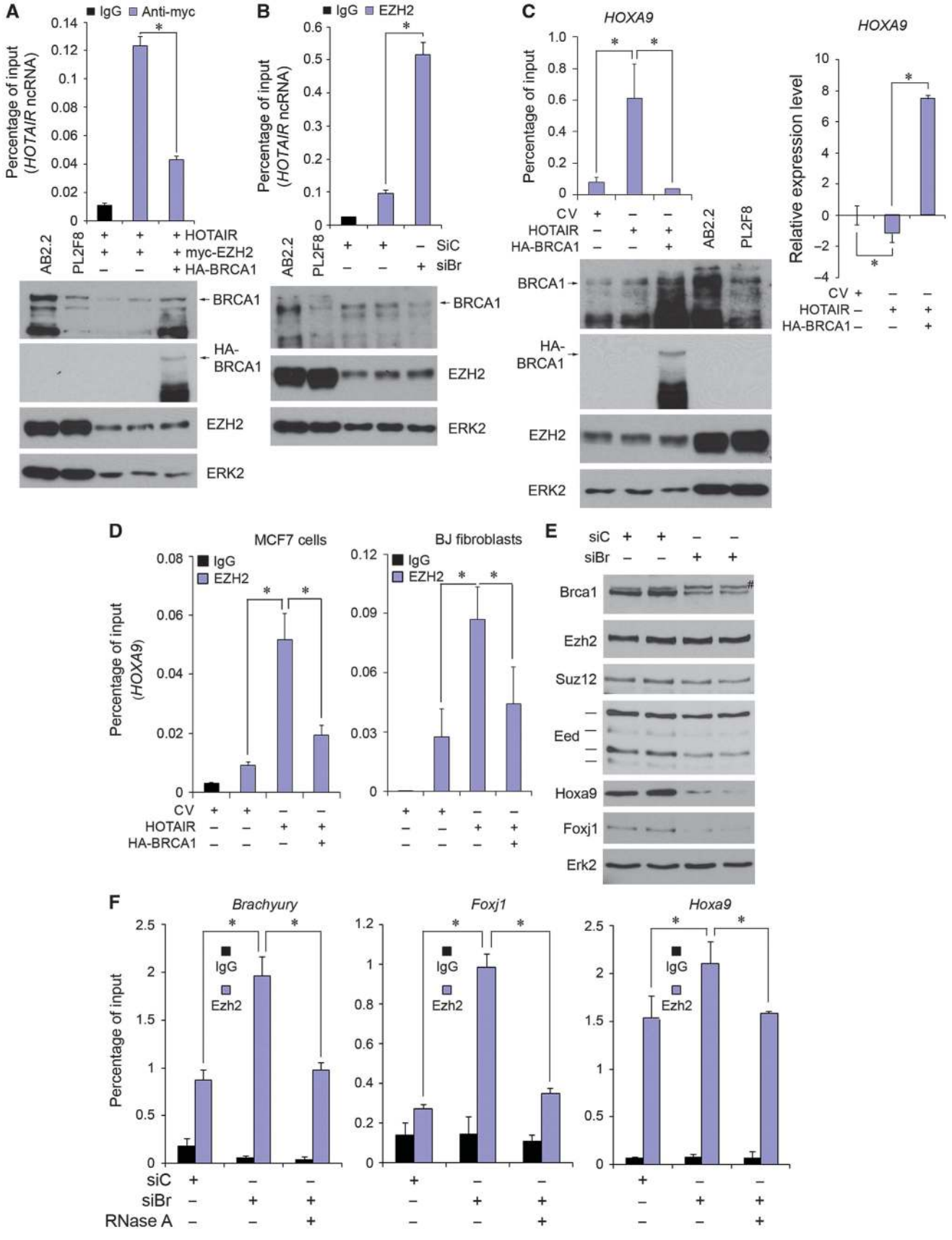

We also investigated how Brca1 affects PRC2 targeting in mouse ES cells. While a recent study demonstrates that the cognate mouse *Hotair* ncRNA is poorly conserved in sequence (Schorderet and Duboule, 2011), genome-wide RIP-seq analysis reveals that there are more than 200 long ncRNAs bound to PRC2 in mouse ES cells (Zhao *et al*, 2010). It is worth noting that pretreatment of nuclear extracts with RNases invariably abolished Ezh2 binding with all the ncRNAs examined (Zhao *et al*, 2010), whereas RNase treatment of nuclear extracts does not generally affect chromatin and nuclei ChIP efficiency (Yap *et al*, 2010). To determine if ncRNAs also play a role in Brca1 regulation of Ezh2 targeting in mouse ES cells, endogenous Brca1 was knocked down by gene-specific siRNAs in R1 ES cells and nuclear extracts were mock treated or treated with RNase A prior to nuclei ChIP assay. Similar to the results obtained in MCF7 cells (Figure 4A), Brca1 knockdown decreased Hoxa9 and Foxj1 protein expression in R1 ES cells (Figure 5E), indicating that Brca1 knockdown affects PRC2 function in these cells. Brca1 knockdown substantially increased Ezh2 binding to *Brachyury*, *Foxj1* and *Hoxa9* promoters (Figure 5F). Importantly, this effect was abolished by RNase A treatment (Figure 5F). These data suggest that Brca1 may regulate PRC2 targeting in mouse ES cells via a mechanism similar to that mediated by *HOTAIR* in human breast cancer cells.

Brca1 affects mouse ES cell differentiation via regulation of Ezh2

PRC2 plays a pivotal role in H3K27me3-mediated silencing of developmental regulators that control human and mouse ES cell differentiation (Boyer *et al*, 2006; Lee *et al*, 2006). We sought to examine whether BRCA1 affects ES cell differentiation via EZH2. R1 mouse ES cells were transfected with control siRNAs or Brca1 and/or Ezh2 siRNA in combination with or without HA-tagged human BRCA1. Cells were then cultured in suspension in the absence of leukemia inhibitory factor (LIF). Cells transfected with control siRNAs underwent differentiation by forming embryoid bodies (EBs) in a time-dependent manner (Figure 6A and B, column 1). Western blot analysis showed that Brca1 was effectively silenced by siRNAs (Figure 6A). No apparent phenotypic difference was detected between Brca1-knockdown and control cells at the early time points (2 days) of culture (Figure 6B, column 2). However, the prolonged (4–8 days) culture severely compromised EB formation in *Brca1*-knockdown cells (Figure 6B, column 2). This effect was rescued by ectopic expression of human BRCA1, which is resistant to mouse Brca1 siRNAs (Figure 6A and B, column 5). Thus, reduced expression of *Brca1* impairs mouse ES cell differentiation. The inhibitory effect of Brca1 was largely diminished by concomitant Ezh2 knockdown

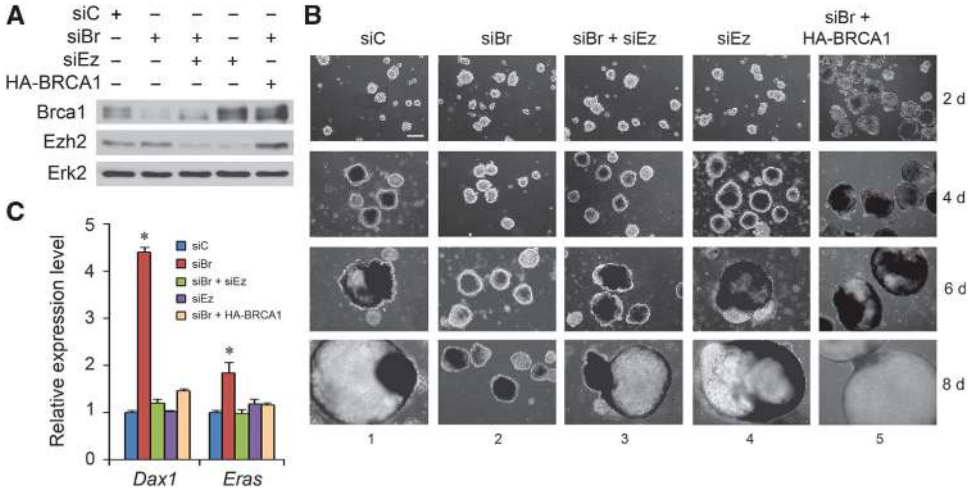

Figure 6 Effect of Brca1 expression on murine ES cell differentiation. (**A**) R1 ES cells were transfected as indicated and subjected to western blot analysis at 48 h after transfection. (**B**) R1 cells were transfected as in (**A**). Cells were cultured on low-attachment plates in the absence of LIF. Images were taken 2, 4, 6 and 8 days after plating. Scale bar, 200 μm. (**C**) R1 cells were transfected as in (**A**). At 6 days after cultured in suspension, cells were harvested for RT–qPCR analysis of expression of stem cell markers *Dax1* and *Eras* (means ± s.d., $n=3$). *$P<0.05$ comparing *Dax1* and *Eras* expression in the siBr-transfected group to every other group. Source data for this figure is available on the online supplementary information page.

Figure 5 BRCA1 regulation of ncRNA-mediated recruitment of EZH2 on its targeting gene loci. (**A**) Effect of BRCA1 overexpression on the binding of *HOTAIR* ncRNA to EZH2. Transfected MCF7 cells were harvested for western blots and RIP with anti-myc or nonspecific IgG. Lysates from AB2.2 and Brca1-heterozygous PL2F8 mouse ESC lines were used as positive/negative controls to define the BRCA1 band on western blots. Retrieved *HOTAIR* ncRNA was analysed by RT–qPCR ($n=3$). *$P<0.01$. (**B**) Effect of BRCA1 knockdown on the binding of *HOTAIR* ncRNA to EZH2. MCF7 cells were transfected with control (siC) and BRCA1-specific siRNAs (siBR) and subjected to western blots and RIP with anti-EZH2 or nonspecific IgG. Retrieved *HOTAIR* ncRNA was analysed by RT–qPCR ($n=3$). *$P<0.01$. (**C**) Effect of BRCA1 on *HOTAIR*-enhanced binding of EZH2 to the *HOXA9* promoter (left) and *HOXA9* mRNA expression (right). MDA-MB-231 cells were transfected with plasmids as indicated and subjected to western blots. The binding of EZH2 to the *HOXA9* promoter was analysed by ChIP using anti-EZH2 antibody (ChIP–qPCR, $n=3$, left) and RT–qPCR ($n=3$, right). * $P<0.01$. (**D**) MCF7 cells and BJ fibroblasts were transfected with the indicated plasmids and subjected to ChIP assay with anti-EZH2 antibody and qPCR analysis ($n=3$). *$P<0.01$. (**E**, **F**) R1 mouse ES cells were transfected with pools of control (siC) or Brca1-specific siRNAs (siBr) and subjected to western blot analysis (**E**). #Nonspecific protein reacted with anti-Brca1 antibody. The other set of cells were harvested for ChIP assay (**F**). Extracted nuclei were pretreated with or without RNase A and subjected to ChIP analysis with anti-Ezh2 antibody. Enrichment of Ezh2 on target loci were analysed by ChIP–qPCR ($n=3$). Data are shown as means ± s.d. from three individual experiments. *$P<0.05$. Source data for this figure is available on the online supplementary information page.

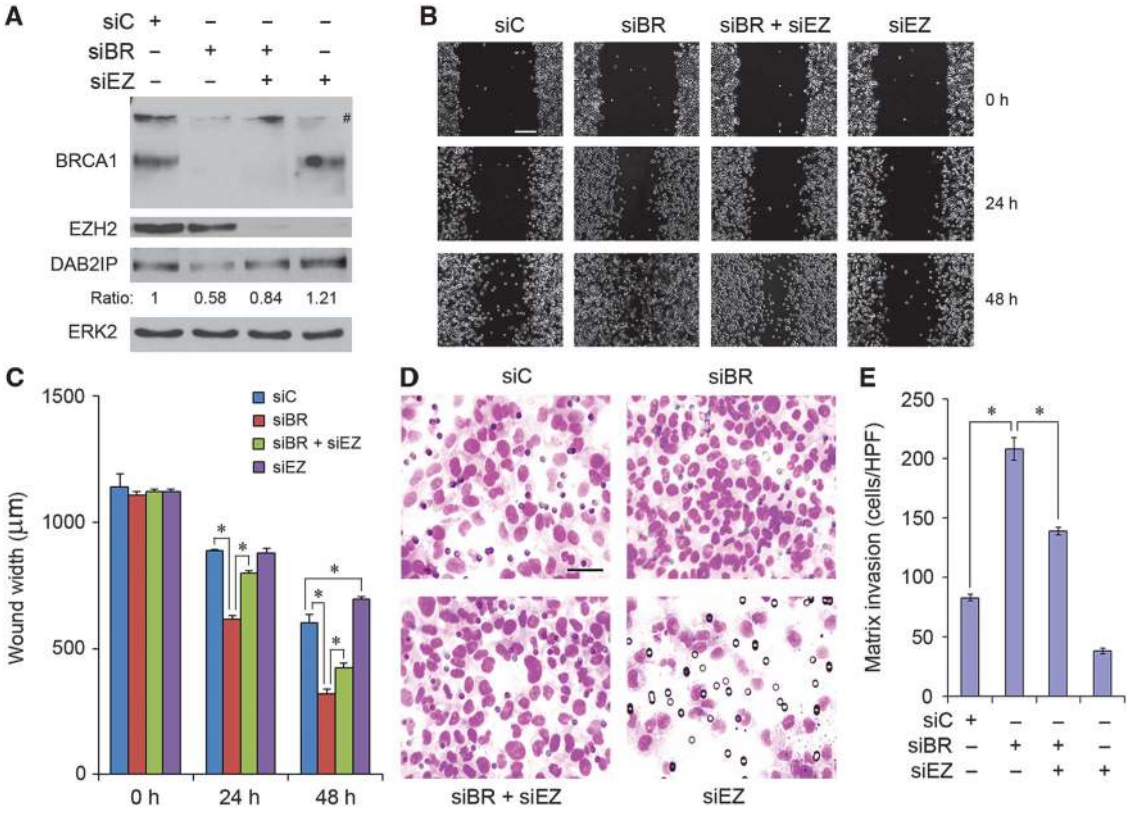

Figure 7 BRCA1 regulates human breast cancer cell migration and invasion via EZH2. (**A**) MDA-MB-231 cells were transfected with HOTAIR and siRNAs as indicated. At 48 h after transfection, one set of cells were harvested and subjected to western blot analysis. #Nonspecific protein reacted with anti-BRCA1 antibody. The density of DAB2IP was determined by normalizing to ERK2 first and then to the normalized value in siC-transfected cells. (**B**, **C**) At 48 h after transfection as in (**A**), artificial wounds were created on cells grown in confluence. Images were taken at 0, 24 and 48 h after wound (**B**). Scale bar, 200 μm. The wound widths were measured and quantified in (**C**) (means ± s.d., $n = 5$). *$P < 0.05$. (**D**, **E**) After transfection as in (**A**), cells were used for transwell invasion assays. Images for invasive cells were taken at 48 h after transfection (**D**). Scale bar, 50 μm. Cell invasion was quantified by measuring the number of invasive cells per high-power field (HPF, ×400) (means ± s.d., $n = 5$) from five random fields (**E**). *$P < 0.01$. Source data for this figure is available on the online supplementary information page.

(Figure 6A and B, column 3). Ezh2 knockdown alone had no drastic effect on EB formation (Figure 6B, column 4). Consistent with the morphology data, expression of stem cell markers *Dax1* and *Eras* (Takahashi *et al*, 2003; Pasini *et al*, 2010) was much higher in *Brca1*-knockdown cells compared to differentiation-unaffected cells in the other four groups (Figure 6C). Together, these data suggest that Ezh2 plays a key role in *Brca1* deficiency-induced blockage of mouse ES cell differentiation.

BRCA1 regulates breast cancer migration and invasion via EZH2

Given that expression of the PRC2 target proteins HOXA9 and DAB2IP is modulated by BRCA1 in MCF7 breast cancer cells (Figure 4A) and that both proteins play important roles in inhibition of cell migration and invasion (Chen *et al*, 2010; Gilbert *et al*, 2010; Xie *et al*, 2010), we sought to determine whether BRCA1 regulates breast cancer cell migration and invasion via EZH2. Treatment of MDA-MB-231 breast cancer cells by a pool of BRCA1-specific siRNAs completely depleted endogenous BRCA1 (Figure 7A). Like in MCF7 cells, BRCA1 silencing decreased DAB2IP protein levels in MDA-MB-231 cells (Figure 7A). Notably, BRCA1 knockdown increased breast cancer cell migration (Figure 7B) and invasion (Figure 7D). The quantified data are shown in Figures 7C and E, respectively. The effect of BRCA1 silencing on DAB2IP expression (Figure 7A), migration (Figure 7B and C) and invasion (Figure 7D and E) was partially reversed by concomitant EZH2 knockdown, suggesting that the effect of BRCA1 on cell migration and invasion is mediated, at least in part, through EZH2. As a control, knockdown of EZH2 alone resulted in a slight increase in DAB2IP expression (Figure 7A), a modest but statistically significant decrease in cell migration (Figure 7B and C) and a marked decrease in invasion (Figure 7D and E). Together, BRCA1 inhibits EZH2-mediated repression of tumour metastasis-inhibitory genes *DAB2IP* and *HOXA9* (Gilbert *et al*, 2010; Xie *et al*, 2010) and blocks EZH2-enhanced migration and invasion of breast cancer cells.

Discussion

The striking bias observed in BRCA1 mutation carriers towards developing aggressive basal-like breast cancers has driven significant interest in understanding how BRCA1 might regulate gene expression and cell fate. Mediating global gene silencing, the PRC2 chromatin-modifying complex has been implicated in stem cell differentiation (Boyer *et al*, 2006; Lee *et al*, 2006; Pasini *et al*, 2007; Ezhkova *et al*, 2009) and cancer progression (Varambally *et al*, 2002; Bracken *et al*, 2003; Kleer *et al*, 2003). In this report we provide evidence that BRCA1 interacts with EZH2 *in vitro* and in cultured cells.

Reduction of BRCA1 levels in ES cells leads to genome-wide re-targeting of EZH2 and concomitant increase in H3K27me3 levels in PRC2 target loci. BRCA1 deficiency also blocks ES cell differentiation and enhances breast cancer cell migration and invasion, and these effects are mediated, at least in part, through EZH2. Thus, we have identified modulation of EZH2 functions as a novel mechanism of BRCA1 in regulation of gene expression, stem cell differentiation and cancer aggressive phenotypes.

BRCA1 is detected in many protein complexes with diverse functions including DNA damage response and repair, transcription regulation and chromatin remodelling (Huen *et al*, 2010). Through the RING domain at the NH2-terminus, BRCA1 forms a heterodimer with BARD1, a well-studied BRCA1 partner protein that has been implicated in regulation of genomic stability, DNA repair and transcription (Meza *et al*, 1999; Huen *et al*, 2010). Our *in vitro* protein binding and co-IP assays demonstrated that BRCA1 binds to the PRC2 complex through its NH2-terminal (amino acids 1–1021), but not the COOH-terminal portion (amino acids 1022–1863). However, we found that neither BARD1 was detected in the BRCA1–PRC2 complex nor BARD1 overexpression affected BRCA1–EZH2 interaction. Thus, our data reveal that BRCA1 associates with PRC2 in a protein complex different from the BRCA1–BARD1 complex, suggesting that BRCA1–PRC2 interaction works independent of the BRCA1–BARD1 heterodimer and thereby may not interfere with the heterodimer function of BRCA1–BARD1 in DNA damage. Moreover, there is an emerging link between PcG and the DNA damage response in mammalian cells (Liu *et al*, 2009; Chou *et al*, 2010; Lukas *et al*, 2011; Vissers *et al*, 2012). We found that the binding of EZH2 by BRCA1 was substantially reduced following UV irradiation in 293T cells (Supplementary Figure S6). These data implicate that BRCA1-mediated inhibition of EZH2 can be attenuated in response to DNA damage, which is consistent with the notion that activated EZH2 might enhance DNA repair by repressing gene transcription at sites of damage (Chou *et al*, 2010; Vissers *et al*, 2012). How DNA damage affects the BRCA1–EZH2 interaction warrants further investigation.

BRCA1 has been implicated in mammary luminal epithelial differentiation and basal-like breast cancer development (Furuta *et al*, 2005; Liu *et al*, 2008; Lim *et al*, 2009; Molyneux *et al*, 2010; Proia *et al*, 2011). However, which biochemical activity of BRCA1 mediates such a function is not fully understood. Using mouse ES cells as a working model, we demonstrate that Brca1 knockdown blocks mouse ES cell differentiation in a manner dependent on Ezh2. We provide evidence that decreased expression of Brca1 broadens genome-wide occupancy of Ezh2 on chromatin and represses Ezh2 target gene expression in mouse ES cell lines. We further show that loss of BRCA1 induces aggressive (migratory/invasive) phenotypes of breast cancer and that these effects are mediated through EZH2. Based upon these results, we envisage a model that reduced BRCA1 expression augments function of PRC2, thereby preventing committed cell lineage differentiation and/or favouring undesired reprogramming of differentiated *BRCA1*-mutated luminal cells into basal-like, aggressive breast adenocarcinoma cells. Our hypothesis is supported by previous findings that the function of PRC2 is crucial for the maintenance of stem cell properties and reprogramming of somatic cells into iPS cells (Boyer *et al*, 2006; Lee *et al*, 2006; Pasini *et al*, 2007; Ezhkova *et al*, 2009; Pereira *et al*, 2010; Onder *et al*, 2012). Moreover, this notion is consistent with the report that the synthetic lethality of BRCA1-mutant breast cancers is attributed to EZH2 inhibition (Puppe *et al*, 2009). It is hence warranted to explore if EZH2 plays a causal role in Brca1 deletion-induced formation of basal-like breast tumours in animals (Liu *et al*, 2007).

Findings from mouse and human ES cell studies suggest that PRC2 plays a key role in maintenance of ES cell pluripotency and H3K27me3-mediated transcriptional repression of cell lineage-specific differentiation genes (Boyer *et al*, 2006; Lee *et al*, 2006). Further studies show that PRC2 targets are bivalent genes that often contain the transcription repression mark H3K27me3 and the activation mark H3K4me3 (Bernstein *et al*, 2006), suggesting that PRC2 target genes are poised for activation during differentiation. Consistent with this notion, it has been shown that Suz12-null mouse ES cells fail to undergo retinoic acid-induced neuronal differentiation (Pasini *et al*, 2007) and Eed-null ES cells exhibit severe defect in mesoendoderm (ME) differentiation (Shen *et al*, 2008). Thus, it has been speculated that PRC2 complexes are required for both suppression and activation of differentiation genes in ES cells (Ezhkova *et al*, 2009). In contrast to the findings in Suz12- and Eed-null ES cells, we found that EZH2 knockdown did not impair ES cell differentiation. Similar to our observation, it has been shown previously that Ezh2-null ES cells have less severe defect in ME differentiation than Eed-null cells (Shen *et al*, 2008). One plausible explanation is that Ezh1, a homologue of Ezh2, has complementary but nonredundant roles in mediating H3K27me3 and ES cell function (Margueron *et al*, 2008; Shen *et al*, 2008). Additionally, different from Ezh2-null ES cells, the residual Ezh2 proteins in Ezh2-knockdown ES cells (Figure 6A) may enable to fine-tune the balance between suppression and activation of differentiation genes.

Although it is not entirely clear how PRC2 targets specific chromatin regions in mammalian cells (Kaneko *et al*, 2010), long ncRNAs *HOTAIR* and *XIST* have been shown to bind to and recruit the PRC2 complex in *cis* or in *trans* (Rinn *et al*, 2007; Zhao *et al*, 2008). A functional motif, designated as ncRBD1, is critical for EZH2 binding to *HOTAIR* and *XIST* (Kaneko *et al*, 2010). Consistent with the observation that the BRCA1 binding region in EZH2 overlaps with ncRBD1, we show that BRCA1 overexpression inhibits, but BRCA1 knockdown enhances, EZH2 binding to *HOTAIR*. BRCA1 overexpression also abolishes *HOTAIR*-augmented binding of EZH2 on the promoter of PRC2 target gene *HOXA9* in human breast cancer cells and fibroblasts. Despite the fact that the cognate mouse *Hotair* ncRNA is poorly conserved in sequence (Schorderet and Duboule, 2011), we provide evidence that Brca1 knockdown-induced Ezh2 recruitment at PRC2 target loci was abolished by RNase treatment in mouse ES cells. Thus, our data suggest that inhibition of EZH2 binding to ncRNAs could be one of the potential mechanisms that mediate BRCA1 interference of PRC2 targeting in both ES and breast cancer cells.

In closing, BRCA1 has been implicated in transcription regulation and mammary luminal epithelial differentiation, and loss of BRCA1 was shown to lead to basal-like breast cancers that are migratory and invasive; however, the underlying mechanism is largely unclear. We uncovered a pre-

viously uncharacterized interaction between the tumour-suppressor BRCA1 and the oncoprotein EZH2. Reduction of BRCA1 levels broadens genome-wide EZH2 occupancy on chromatin and elevates H3K27me3 levels at PRC2 target loci. We further showed that decreased BRCA1 expression blocks ES cell differentiation and augments breast cancer migration and invasion in a manner dependent on EZH2. Thus, our study has identified the BRCA1–EZH2 interaction as a key mechanism mediating BRCA1 regulation of gene expression, stem cell differentiation and cancer aggressive phenotypes. Our findings suggest that the PRC2 complex may serve as a viable target for the treatment of human basal-like breast cancers carrying a mutated or methylated *BRCA1* gene.

Materials and methods

Plasmids

Myc-tagged EZH2 plasmid was kindly provided by Mien-Chie Hung (the University of Texas M. D. Anderson Cancer Center, Houston, TX, USA). Baculovirus expression vectors for mouse Ezh2, human SUZ12, EED and RbAp48 were kindly provided by Yi Zhang (the University of North Carolina, Chapel Hill, NC, USA). Mouse Ezh1 was kindly provided by Xiaohua Shen (Tsinghua University, Beijing, China). The mammalian expression vector for HA-tagged BRCA1 was kindly provided by Fergus Couch (Mayo Clinic College of Medicine, Rochester, MN, USA). V5-tagged expression vectors for wild-type BRCA1, BRCA1-N (amino acids 1–1100), were constructed by PCR amplifying and subcloning the corresponding fragments of BRCA1 into pcDNA3.1D vector (Invitrogen). A series of BRCA1 fragments (1–304, 252–551, 501–1021, 1022–1500 and 1051–1863) and EZH2 (1–173, 174–340, 341–559 and 560–751) were amplified by PCR and subcloned into pGEX-4T-1 vector (GE Healthcare) for construction of recombinant GST-BRCA1 and GST-EZH2 fusion proteins, respectively. The FLAG-BARD1 expression vector was kindly provided by Zhenkun Lou (Mayo Clinic, Rochester, MN, USA). The retrovirus-based *HOTAIR* expression vector LZRS-HOTAIR constructed by the laboratory of Howard Chang (Stanford University School of Medicine, Stanford, CA, USA) (Gupta *et al*, 2010) was obtained from Addgene and subcloned into the backbone vector pcDNA3.1 (Invitrogen).

Antibodies and reagents

Antibodies used are as follows: rabbit polyclonal anti-BRCA1 antibody was described previously (Yu *et al*, 2003); anti-EZH2 (XP) (Cell Signaling Technology); anti-EED, anti-SUZ12 (3C1.2) (Millipore); anti-HOXA9, anti-DAB2IP, anti-H3 (total), anti-H3K27me3 (Abcam); anti-SUZ12 (D-10), anti-myc, anti-ERK2 (Santa Cruz Biotechnology); anti-FOXJ1, anti-HA (Covance); and anti-FLAG (Sigma Aldrich). Antibodies against total and phosphorylated CHK1 were kindly provided by Zhenkun Lou (Mayo Clinic).

Cell culture and transfection

MCF7, MDA-MB-231, 293T and BJ cells were cultured in Dulbecco's modified Eagle's medium (DMEM; Invitrogen) supplemented with 10% fetal bovine serum (FBS; Hyclone). MCF10A cells were cultured in DMEM/F12 supplemented with 5% horse serum (Invitrogen), 1% penicillin/streptomycin (Invitrogen), 0.5 μg/ml hydrocortisone (Sigma), 100 ng/ml cholera toxin (Sigma), 10 μg/ml insulin (Sigma) and 20 ng/ml recombinant human EGF (Peprotech). Mouse wild-type (AB2.2), *Brca1*-heterozygous mutant (PL2F8) and human *BRCA1*-rescued PL2F8 (PL2F8-BAC) ES cell lines were kindly provided by Shyam K Sharan (Chang *et al*, 2009). R1 mouse ES cell line was purchased from ATCC. Mouse ES cells were cultured in KNOCKOUT^{TM} DMEM medium (Invitrogen) supplemented with 15% ES cell-screened FBS (Hyclone), 0.1 mM 2-mercaptoethanol, 1 mM L-glutamine (Invitrogen) and 10^3 unit/ml LIF (Millipore) on 0.1% gelatin-coated dishes. Cells were cultured at 37°C supplied with 5% CO_2. Transfection of cells was performed by electroporation using an Electro Square Porator ECM 830 (BTX) as we described previously (Huang *et al*, 2006) or using Lipofectamine 2000 (Invitrogen). Approximately 75–90% transfection efficiencies were routinely achieved (Huang *et al*, 2006).

RNA interference

siRNAs for human *BRCA1* (siBR #1, 5′-GGGAUACCAUGCAACAUAA-3′ and siBR #2, 5′-CUAGAAAUCUGUUGCUAUG-3′), smart pools of siRNAs against human *BRCA1* and *EZH2*, mouse *Brca1* and *Ezh2* and nonspecific control siRNAs were purchased from Dharmacon. siRNA for human *HOTAIR* (siHOTAIR GAACGGGAGUACAGAG AGAUU) was synthesized by Dharmacon. siRNA transfection of cells was performed following the manufacturer's instruction.

RT–qPCR

Total RNA was isolated from cells and cDNA was synthesized using the Super-Script kit from Invitrogen. Two-step real-time PCR was performed using the SYBR Green Mix (Bio-Rad) and an iCycler iQTM system (Bio-Rad) as we described previously (Huang *et al*, 2006). Both forward and reverse primers were used at a final concentration of 200 nM. The primer sequences used for PCR are described in Supplementary Table S2.

Co-immunoprecipitation and western blotting

Immunoprecipitations were performed as described previously (van der Vlag and Otte, 1999; Huang *et al*, 2006; Pasini *et al*, 2008). Briefly, cells were harvested and lysed using glass Dounce homogenizer in cell lysis buffer (50 mM Tris–HCl, pH 7.5, 150 mM NaCl, 1% Nonidet P-40, 0.5% sodium deoxycholate and 1% protease inhibitor cocktails; Sigma Aldrich). Ethidium bromide was added to a final concentration of 50 μg/ml to disrupt DNA–protein interactions in endogenous protein co-IP experiments. Cell lysis was centrifuged and the supernatant (5 ~ 10 mg) was incubated with indicated antibodies (5–10 μg) and protein-G beads (Invitrogen) at 4°C overnight. The beads were washed five times with cell lysis buffer and the precipitated proteins were subjected to western blot analysis. For RNase A treatment, cell lysates were mock treated or treated with 50 μg/ml RNase A at 37°C for 10 min and then subjected to co-IP experiments as described above. For western blotting, protein samples were prepared by lysing cells in lysis buffer (1% Nonidet P-40 and 0.1% SDS in 1 × PBS solution plus protease inhibitors). Equal amounts of proteins (50–100 μg) from cell lysates were denatured in sample buffer (Invitrogen), subjected to SDS–polyacrylamide gel electrophoresis and were transferred to nitrocellulose membranes (Bio-Rad). The membranes were immunoblotted with specific primary antibodies, horseradish peroxidase-conjugated secondary antibodies and visualized by SuperSignal West Pico Stable Peroxide Solution (Thermo Scientific).

ChIP and RIP assays

ChIP assay was performed as previously described (Boyer *et al*, 2005). Briefly, cells were crosslinked with 1% formaldehyde for 10 min at room temperature. Crosslinking was quenched by adding 2.5 M glycine to a final concentration of 125 mM. Cells were scraped and washed twice with 1 × PBS. Cell nuclei were extracted by resuspending cells in lysis buffer 1 (50 mM HEPES, pH 7.5, 140 mM NaCl, 1 mM EDTA, 10% glycerol, 0.5% Nonidet P-40 and 0.25% Triton X-100) for 10 min at 4°C and lysis buffer 2 (10 mM Tris–HCl, pH 8.0, 200 mM NaCl and 1 mM EDTA) for 10 min at room temperature. Cell nuclei were lysed with lysis buffer 3 (10 mM Tris–HCl, pH 8.0, 100 mM NaCl, 1 mM EDTA and 0.1% sodium deoxycholate) and sonicated to solubilize and shear crosslinked DNA. Cell lysis was centrifuged and the supernatant was incubated overnight at 4°C with 30 μl protein G beads (Invitrogen) that has been preincubated with 10 μg of indicated antibody. The beads were washed seven times with radioimmune precipitation buffer (RIPA) buffer (50 mM HEPES-KOH, pH 7.6, 500 mM LiCl, 1 mM EDTA, 1% NP-40 and 0.7% Na-Deoxycholate) and one time with TE containing 50 mM NaCl. The precipitated DNA was eluted by heating at 65°C and crosslinking was reversed by overnight incubation at 65°C. The ChIP DNA was extracted with a PCR purification kit (Qiagen) and was subjected to real-time PCR amplification using the primers specific for the promoters of genes analysed (Supplementary Table S2). The data for the occupation are expressed as a ratio of the cycle threshold for the immunoprecipitated chromatin DNA versus the cycle threshold for the input (5%) samples and further normalized to the values in control cells. RIP was performed as described previously (Kaneko *et al*, 2010).

ChIP-chip assay

Fragmented DNA obtained from ChIP assay was repaired by DNA Terminator End Repair Kit (Lucigen Corporation, Middleton, WI) and purified by QIAquick PCR purification kit as described previously (Murphy *et al*, 2010). Then, two unidirectional linkers were annealed (JW102 5′-GCGGTGACCCGGGAGATCTGAATTC-3′; JW103 5′-GAATTCAGATC-3′) and were ligated to the blunt end DNA at 16 °C overnight. The purified products were amplified to 2 μg by LM–PCR as described previously (Murphy *et al*, 2010). NimbleGen Mouse ChIP-chip 3 × 720K RefSeq Promoter Arrays (Roche) were used for hybridization. Relative enrichments were calculated by dividing the normalized level of ChIP DNA to that of input DNA at corresponding locus. To identify DNA promoter regions with significant association, the enrichment for each probe on the array was calculated as the ratio of the intensities of the ChIP product (Cy5) to control input chromatin (Cy3). Probes covered 4000 bp for each of 20 404 promoter proximal regions in the mouse genome (MM9).

Nuclear ChIP assay

Prior to ChIP assay, nuclear extraction and RNase A treatment were performed as previously described (Yap *et al*, 2010). Briefly, R1 mouse ES cells were transfected with Brca1-specific siRNA or control siRNA (Dharmacon). At 48 h post transfection, cell nuclei were extracted using cell membrane lysis buffer (10 mM HEPES, pH 8.0, 1.5 mM $MgCl_2$, 0.5 mM DTT, 0.01% Nonidet P-40 and 1% protease inhibitor cocktails) and treated in TMS buffer (50 mM Tris–HCl, pH 8.0, 100 mM NaCl, 10 mM $MgCl_2$) with or without 50 μg/ml RNase A (Invitrogen) at room temperature for 30 min. Then, cell nuclei were crosslinked with 1% formaldehyde and subjected to ChIP assay as described above.

Embryoid body formation assay

Embryoid body formation assays were performed as described previously (Li *et al*, 2010). Briefly, cells were plated at a density of 3×10^5 per 10-cm Ultra-low-Attachment Dishes (Corning) containing 15 ml of ES medium without LIF, and the medium was changed every other day. The pictures of embryoid body formation were taken every other day.

Wound healing assay

MDA-MB-231 cells were transiently transfected with pools of BRCA1-specific siRNA, EZH2-specific siRNA or control siRNA (Dharmacon) as indicated. Artificial wounds were created on the cell monolayer when cells were grown to confluence. Migrated cells and wound healing were visualized at 0, 24 and 48 h. For each group, at least three artificial wounds were photographed immediately and at the time points indicated after the wound formation. Cell migration was evaluated by measuring the difference in wound width.

In vitro invasion assay

In vitro invasion assay was conducted by using BioCoat Matrigel invasion chamber (BD Biosciences) according to the manufacturer's protocol. MDA-MB-231 cells were transfected with BRCA1-specific siRNA, EZH2-specific siRNA or control siRNA as indicated, cultured in the insert for 48 h and stained with Diff-Quick stain. At least five fields for each group were photographed after staining. Invasion was evaluated by counting the number of the invaded cells.

Statistics

Experiments were carried out with three or more replicates. Statistical analyses were performed using two-tailed Student's *t*-test. $P < 0.05$ is considered statistically significant. Hypergeometric test was used to determine the statistical significance of the EZH2 new target genes overlapped between PL2F8 cells with *Brca1*-heterozygous deletion and *Brca1*-knockdown R1 cells.

Supplementary data

Supplementary data are available at *The EMBO Journal* Online (http://www.embojournal.org).

Acknowledgements

We thank Mien-Chie Hung, Yi Zhang, Zhenkun Lou, Xiaohua Shen and Fergus Couch for plasmids and reagents; Shyam Sharan for matched Brca1 wild-type, deficient and rescued mouse ES cells; and Jeffrey Simon and Aswathy Rai for providing purified PRC2 complexes. This work was supported in part by grants from the National Institutes of Health (CA134514 and CA130908 to HH and K99/R00CA129565 to JY), the Department of Defense (W81XWH-09-1-622 to HH) and the American Cancer Society (the Research Scholar Award RSG-12-085-01 to JY).

Author contributions: LW (Lan Wang), XZ, SC, LD and JZ (Jian Zhong) performed the experiments described in the manuscript. JCZ, LW (Liguo Wang), AS, JZ (Jizu Zhi) and JY performed ChIP-chip data and statistical analyses. AK performed mass spectrometry and data analysis. YM and JC provide reagents. HH conceived the study. LW (Lan Wang), XZ, SC, YM, JC and HH wrote the paper.

Conflict of interest

The authors declare that they have no conflict of interest.

References

Ben-Porath I, Thomson MW, Carey VJ, Ge R, Bell GW, Regev A, Weinberg RA (2008) An embryonic stem cell-like gene expression signature in poorly differentiated aggressive human tumors. *Nat Genet* **40:** 499–507

Bernstein BE, Mikkelsen TS, Xie X, Kamal M, Huebert DJ, Cuff J, Fry B, Meissner A, Wernig M, Plath K, Jaenisch R, Wagschal A, Feil R, Schreiber SL, Lander ES (2006) A bivalent chromatin structure marks key developmental genes in embryonic stem cells. *Cell* **125:** 315–326

Bochar DA, Wang L, Beniya H, Kinev A, Xue Y, Lane WS, Wang W, Kashanchi F, Shiekhattar R (2000) BRCA1 is associated with a human SWI/SNF-related complex: linking chromatin remodeling to breast cancer. *Cell* **102:** 257–265

Bohrer LR, Chen S, Hallstrom TC, Huang H (2010) Androgens suppress EZH2 expression via retinoblastoma (RB) and p130-dependent pathways: a potential mechanism of androgen-refractory progression of prostate cancer. *Endocrinology* **151:** 5136–5145

Boyer LA, Lee TI, Cole MF, Johnstone SE, Levine SS, Zucker JP, Guenther MG, Kumar RM, Murray HL, Jenner RG, Gifford DK, Melton DA, Jaenisch R, Young RA (2005) Core transcriptional regulatory circuitry in human embryonic stem cells. *Cell* **122:** 947–956

Boyer LA, Plath K, Zeitlinger J, Brambrink T, Medeiros LA, Lee TI, Levine SS, Wernig M, Tajonar A, Ray MK, Bell GW, Otte AP, Vidal M, Gifford DK, Young RA, Jaenisch R (2006) Polycomb complexes repress developmental regulators in murine embryonic stem cells. *Nature* **441:** 349–353

Bracken AP, Pasini D, Capra M, Prosperini E, Colli E, Helin K (2003) EZH2 is downstream of the pRB-E2F pathway, essential for proliferation and amplified in cancer. *EMBO J* **22:** 5323–5335

Cao R, Wang L, Wang H, Xia L, Erdjument-Bromage H, Tempst P, Jones RS, Zhang Y (2002) Role of histone H3 lysine 27 methylation in Polycomb-group silencing. *Science* **298:** 1039–1043

Caretti G, Di Padova M, Micales B, Lyons GE, Sartorelli V (2004) The Polycomb Ezh2 methyltransferase regulates muscle gene expression and skeletal muscle differentiation. *Genes Dev* **18:** 2627–2638

Cha TL, Zhou BP, Xia W, Wu Y, Yang CC, Chen CT, Ping B, Otte AP, Hung MC (2005) Akt-mediated phosphorylation of EZH2 suppresses methylation of lysine 27 in histone H3. *Science* **310:** 306–310

Chang S, Biswas K, Martin BK, Stauffer S, Sharan SK (2009) Expression of human BRCA1 variants in mouse ES cells allows functional analysis of BRCA1 mutations. *J Clin Invest* **119:** 3160–3171

Chapman MS, Verma IM (1996) Transcriptional activation by BRCA1. *Nature* **382:** 678–679

Chen S, Bohrer LR, Rai AN, Pan Y, Gan L, Zhou X, Bagchi A, Simon JA, Huang H (2010) Cyclin-dependent kinases regulate epigenetic

gene silencing through phosphorylation of EZH2. *Nat Cell Biol* **12:** 1108–1114

Chou DM, Adamson B, Dephoure NE, Tan X, Nottke AC, Hurov KE, Gygi SP, Colaiacovo MP, Elledge SJ (2010) A chromatin localization screen reveals poly (ADP ribose)-regulated recruitment of the repressive polycomb and NuRD complexes to sites of DNA damage. *Proc Natl Acad Sci USA* **107:** 18475–18480

Cortez D, Wang Y, Qin J, Elledge SJ (1999) Requirement of ATM-dependent phosphorylation of brca1 in the DNA damage response to double-strand breaks. *Science* **286:** 1162–1166

Czermin B, Melfi R, McCabe D, Seitz V, Imhof A, Pirrotta V (2002) Drosophila enhancer of Zeste/ESC complexes have a histone H3 methyltransferase activity that marks chromosomal Polycomb sites. *Cell* **111:** 185–196

Ezhkova E, Pasolli HA, Parker JS, Stokes N, Su IH, Hannon G, Tarakhovsky A, Fuchs E (2009) Ezh2 orchestrates gene expression for the stepwise differentiation of tissue-specific stem cells. *Cell* **136:** 1122–1135

Foulkes WD (2004) BRCA1 functions as a breast stem cell regulator. *J Med Genet* **41:** 1–5

Foulkes WD, Stefansson IM, Chappuis PO, Begin LR, Goffin JR, Wong N, Trudel M, Akslen LA (2003) Germline BRCA1 mutations and a basal epithelial phenotype in breast cancer. *J Natl Cancer Inst* **95:** 1482–1485

Furuta S, Jiang X, Gu B, Cheng E, Chen PL, Lee WH (2005) Depletion of BRCA1 impairs differentiation but enhances proliferation of mammary epithelial cells. *Proc Natl Acad Sci USA* **102:** 9176–9181

Gilbert PM, Mouw JK, Unger MA, Lakins JN, Gbegnon MK, Clemmer VB, Benezra M, Licht JD, Boudreau NJ, Tsai KK, Welm AL, Feldman MD, Weber BL, Weaver VM (2010) HOXA9 regulates BRCA1 expression to modulate human breast tumor phenotype. *J Clin Invest* **120:** 1535–1550

Gupta RA, Shah N, Wang KC, Kim J, Horlings HM, Wong DJ, Tsai MC, Hung T, Argani P, Rinn JL, Wang Y, Brzoska P, Kong B, Li R, West RB, van de Vijver MJ, Sukumar S, Chang HY (2010) Long non-coding RNA HOTAIR reprograms chromatin state to promote cancer metastasis. *Nature* **464:** 1071–1076

Harkin DP, Bean JM, Miklos D, Song YH, Truong VB, Englert C, Christians FC, Ellisen LW, Maheswaran S, Oliner JD, Haber DA (1999) Induction of GADD45 and JNK/SAPK-dependent apoptosis following inducible expression of BRCA1. *Cell* **97:** 575–586

Huang H, Regan KM, Lou Z, Chen J, Tindall DJ (2006) CDK2-dependent phosphorylation of FOXO1 as an apoptotic response to DNA damage. *Science* **314:** 294–297

Huen MS, Sy SM, Chen J (2010) BRCA1 and its toolbox for the maintenance of genome integrity. *Nat Rev Mol Cell Biol* **11:** 138–148

Kaneko S, Li G, Son J, Xu CF, Margueron R, Neubert TA, Reinberg D (2010) Phosphorylation of the PRC2 component Ezh2 is cell cycle-regulated and up-regulates its binding to ncRNA. *Genes Dev* **24:** 2615–2620

Kennison JA (1995) The Polycomb and trithorax group proteins of Drosophila: trans-regulators of homeotic gene function. *Annu Rev Genet* **29:** 289–303

King MC, Marks JH, Mandell JB (2003) Breast and ovarian cancer risks due to inherited mutations in BRCA1 and BRCA2. *Science* **302:** 643–646

Kleer CG, Cao Q, Varambally S, Shen R, Ota I, Tomlins SA, Ghosh D, Sewalt RG, Otte AP, Hayes DF, Sabel MS, Livant D, Weiss SJ, Rubin MA, Chinnaiyan AM (2003) EZH2 is a marker of aggressive breast cancer and promotes neoplastic transformation of breast epithelial cells. *Proc Natl Acad Sci USA* **100:** 11606–11611

Ku M, Koche RP, Rheinbay E, Mendenhall EM, Endoh M, Mikkelsen TS, Presser A, Nusbaum C, Xie X, Chi AS, Adli M, Kasif S, Ptaszek LM, Cowan CA, Lander ES, Koseki H, Bernstein BE (2008) Genomewide analysis of PRC1 and PRC2 occupancy identifies two classes of bivalent domains. *PLoS Genet* **4:** e1000242

Kuzmichev A, Nishioka K, Erdjument-Bromage H, Tempst P, Reinberg D (2002) Histone methyltransferase activity associated with a human multiprotein complex containing the Enhancer of Zeste protein. *Genes Dev* **16:** 2893–2905

Lai Z, Freedman DA, Levine AJ, McLendon GL (1998) Metal and RNA binding properties of the hdm2 RING finger domain. *Biochemistry (Mosc)* **37:** 17005–17015

Lakhani SR, Reis-Filho JS, Fulford L, Penault-Llorca F, van der Vijver M, Parry S, Bishop T, Benitez J, Rivas C, Bignon YJ, Chang-Claude J, Hamann U, Cornelisse CJ, Devilee P, Beckmann MW, Nestle-Kramling C, Daly PA, Haites N, Varley J, Lalloo F *et al* (2005) Prediction of BRCA1 status in patients with breast cancer using estrogen receptor and basal phenotype. *Clin Cancer Res* **11:** 5175–5180

Landeira D, Sauer S, Poot R, Dvorkina M, Mazzarella L, Jorgensen HF, Pereira CF, Leleu M, Piccolo FM, Spivakov M, Brookes E, Pombo A, Fisher C, Skarnes WC, Snoek T, Bezstarosti K, Demmers J, Klose RJ, Casanova M, Tavares L *et al* (2010) Jarid2 is a PRC2 component in embryonic stem cells required for multi-lineage differentiation and recruitment of PRC1 and RNA Polymerase II to developmental regulators. *Nat Cell Biol* **12:** 618–624

Lee TI, Jenner RG, Boyer LA, Guenther MG, Levine SS, Kumar RM, Chevalier B, Johnstone SE, Cole MF, Isono K, Koseki H, Fuchikami T, Abe K, Murray HL, Zucker JP, Yuan B, Bell GW, Herbolsheimer E, Hannett NM, Sun K *et al* (2006) Control of developmental regulators by Polycomb in human embryonic stem cells. *Cell* **125:** 301–313

Li G, Margueron R, Ku M, Chambon P, Bernstein BE, Reinberg D (2010) Jarid2 and PRC2, partners in regulating gene expression. *Genes Dev* **24:** 368–380

Lim E, Vaillant F, Wu D, Forrest NC, Pal B, Hart AH, Asselin-Labat ML, Gyorki DE, Ward T, Partanen A, Feleppa F, Huschtscha LI, Thorne HJ, Fox SB, Yan M, French JD, Brown MA, Smyth GK, Visvader JE, Lindeman GJ (2009) Aberrant luminal progenitors as the candidate target population for basal tumor development in BRCA1 mutation carriers. *Nat Med* **15:** 907–913

Liu J, Cao L, Chen J, Song S, Lee IH, Quijano C, Liu H, Keyvanfar K, Chen H, Cao LY, Ahn BH, Kumar NG, Rovira II, Xu XL, van Lohuizen M, Motoyama N, Deng CX, Finkel T (2009) Bmi1 regulates mitochondrial function and the DNA damage response pathway. *Nature* **459:** 387–392

Liu S, Ginestier C, Charafe-Jauffret E, Foco H, Kleer CG, Merajver SD, Dontu G, Wicha MS (2008) BRCA1 regulates human mammary stem/progenitor cell fate. *Proc Natl Acad Sci USA* **105:** 1680–1685

Liu X, Holstege H, van der Gulden H, Treur-Mulder M, Zevenhoven J, Velds A, Kerkhoven RM, van Vliet MH, Wessels LF, Peterse JL, Berns A, Jonkers J (2007) Somatic loss of BRCA1 and p53 in mice induces mammary tumors with features of human BRCA1-mutated basal-like breast cancer. *Proc Natl Acad Sci USA* **104:** 12111–12116

Lukas J, Lukas C, Bartek J (2011) More than just a focus: the chromatin response to DNA damage and its role in genome integrity maintenance. *Nat Cell Biol* **13:** 1161–1169

Margueron R, Li G, Sarma K, Blais A, Zavadil J, Woodcock CL, Dynlacht BD, Reinberg D (2008) Ezh1 and Ezh2 maintain repressive chromatin through different mechanisms. *Mol Cell* **32:** 503–518

Margueron R, Reinberg D (2011) The Polycomb complex PRC2 and its mark in life. *Nature* **469:** 343–349

Meza JE, Brzovic PS, King MC, Klevit RE (1999) Mapping the functional domains of BRCA1. Interaction of the ring finger domains of BRCA1 and BARD1. *J Biol Chem* **274:** 5659–5665

Miki Y, Swensen J, Shattuck-Eidens D, Futreal PA, Harshman K, Tavtigian S, Liu Q, Cochran C, Bennett LM, Ding W *et al.* (1994) A strong candidate for the breast and ovarian cancer susceptibility gene BRCA1. *Science* **266:** 66–71

Molyneux G, Geyer FC, Magnay FA, McCarthy A, Kendrick H, Natrajan R, Mackay A, Grigoriadis A, Tutt A, Ashworth A, Reis-Filho JS, Smalley MJ (2010) BRCA1 basal-like breast cancers originate from luminal epithelial progenitors and not from basal stem cells. *Cell Stem Cell* **7:** 403–417

Morin RD, Johnson NA, Severson TM, Mungall AJ, An J, Goya R, Paul JE, Boyle M, Woolcock BW, Kuchenbauer F, Yap D, Humphries RK, Griffith OL, Shah S, Zhu H, Kimbara M, Shashkin P, Charlot JF, Tcherpakov M, Corbett R *et al* (2010) Somatic mutations altering EZH2 (Tyr641) in follicular and diffuse large B-cell lymphomas of germinal-center origin. *Nat Genet* **42:** 181–185

Muller J, Hart CM, Francis NJ, Vargas ML, Sengupta A, Wild B, Miller EL, O'Connor MB, Kingston RE, Simon JA (2002) Histone

methyltransferase activity of a Drosophila Polycomb group repressor complex. *Cell* **111:** 197–208

Murphy MW, Sarver AL, Rice D, Hatzi K, Ye K, Melnick A, Heckert LL, Zarkower D, Bardwell VJ (2010) Genome-wide analysis of DNA binding and transcriptional regulation by the mammalian Doublesex homolog DMRT1 in the juvenile testis. *Proc Natl Acad Sci USA* **107:** 13360–13365

Onder TT, Kara N, Cherry A, Sinha AU, Zhu N, Bernt KM, Cahan P, Marcarci BO, Unternaehrer J, Gupta PB, Lander ES, Armstrong SA, Daley GQ (2012) Chromatin-modifying enzymes as modulators of reprogramming. *Nature* **483:** 598–602

Pasini D, Bracken AP, Hansen JB, Capillo M, Helin K (2007) The polycomb group protein Suz12 is required for embryonic stem cell differentiation. *Mol Cell Biol* **27:** 3769–3779

Pasini D, Cloos PA, Walfridsson J, Olsson L, Bukowski JP, Johansen JV, Bak M, Tommerup N, Rappsilber J, Helin K (2010) JARID2 regulates binding of the Polycomb repressive complex 2 to target genes in ES cells. *Nature* **464:** 306–310

Pasini D, Hansen KH, Christensen J, Agger K, Cloos PA, Helin K (2008) Coordinated regulation of transcriptional repression by the RBP2 H3K4 demethylase and Polycomb-Repressive Complex 2. *Genes Dev* **22:** 1345–1355

Peng JC, Valouev A, Swigut T, Zhang J, Zhao Y, Sidow A, Wysocka J (2009) Jarid2/Jumonji coordinates control of PRC2 enzymatic activity and target gene occupancy in pluripotent cells. *Cell* **139:** 1290–1302

Pereira CF, Piccolo FM, Tsubouchi T, Sauer S, Ryan NK, Bruno L, Landeira D, Santos J, Banito A, Gil J, Koseki H, Merkenschlager M, Fisher AG (2010) ESCs require PRC2 to direct the successful reprogramming of differentiated cells toward pluripotency. *Cell Stem Cell* **6:** 547–556

Proia TA, Keller PJ, Gupta PB, Klebba I, Jones AD, Sedic M, Gilmore H, Tung N, Naber SP, Schnitt S, Lander ES, Kuperwasser C (2011) Genetic predisposition directs breast cancer phenotype by dictating progenitor cell fate. *Cell Stem Cell* **8:** 149–163

Puppe J, Drost R, Liu X, Joosse SA, Evers B, Cornelissen-Steijger P, Nederlof P, Yu Q, Jonkers J, van Lohuizen M, Pietersen AM (2009) BRCA1-deficient mammary tumor cells are dependent on EZH2 expression and sensitive to Polycomb Repressive Complex 2-inhibitor 3-deazaneplanocin A. *Breast Cancer Res* **11:** R63

Rinn JL, Kertesz M, Wang JK, Squazzo SL, Xu X, Brugmann SA, Goodnough LH, Helms JA, Farnham PJ, Segal E, Chang HY (2007) Functional demarcation of active and silent chromatin domains in human HOX loci by noncoding RNAs. *Cell* **129:** 1311–1323

Schorderet P, Duboule D (2011) Structural and functional differences in the long non-coding RNA hotair in mouse and human. *PLoS Genet* **7:** e1002071

Schwartz YB, Pirrotta V (2007) Polycomb silencing mechanisms and the management of genomic programmes. *Nat Rev Genet* **8:** 9–22

Scully R, Chen J, Ochs RL, Keegan K, Hoekstra M, Feunteun J, Livingston DM (1997) Dynamic changes of BRCA1 subnuclear location and phosphorylation state are initiated by DNA damage. *Cell* **90:** 425–435

Shen X, Kim W, Fujiwara Y, Simon MD, Liu Y, Mysliwiec MR, Yuan GC, Lee Y, Orkin SH (2009) Jumonji modulates polycomb activity and self-renewal versus differentiation of stem cells. *Cell* **139:** 1303–1314

Shen X, Liu Y, Hsu YJ, Fujiwara Y, Kim J, Mao X, Yuan GC, Orkin SH (2008) EZH1 mediates methylation on histone H3 lysine 27 and complements EZH2 in maintaining stem cell identity and executing pluripotency. *Mol Cell* **32:** 491–502

Simon JA, Kingston RE (2009) Mechanisms of polycomb gene silencing: knowns and unknowns. *Nat Rev Mol Cell Biol* **10:** 697–708

Simpson EM, Linder CC, Sargent EE, Davisson MT, Mobraaten LE, Sharp JJ (1997) Genetic variation among 129 substrains and its importance for targeted mutagenesis in mice. *Nat Genet* **16:** 19–27

Sorlie T, Tibshirani R, Parker J, Hastie T, Marron JS, Nobel A, Deng S, Johnsen H, Pesich R, Geisler S, Demeter J, Perou CM, Lonning PE, Brown PO, Borresen-Dale AL, Botstein D (2003) Repeated observation of breast tumor subtypes in independent gene expression data sets. *Proc Natl Acad Sci USA* **100:** 8418–8423

Takahashi K, Mitsui K, Yamanaka S (2003) Role of ERas in promoting tumour-like properties in mouse embryonic stem cells. *Nature* **423:** 541–545

Threadgill DW, Yee D, Matin A, Nadeau JH, Magnuson T (1997) Genealogy of the 129 inbred strains: 129/SvJ is a contaminated inbred strain. *Mamm Genome* **8:** 390–393

van der Vlag J, Otte AP (1999) Transcriptional repression mediated by the human polycomb-group protein EED involves histone deacetylation. *Nat Genet* **23:** 474–478

Varambally S, Cao Q, Mani RS, Shankar S, Wang X, Ateeq B, Laxman B, Cao X, Jing X, Ramnarayanan K, Brenner JC, Yu J, Kim JH, Han B, Tan P, Kumar-Sinha C, Lonigro RJ, Palanisamy N, Maher CA, Chinnaiyan AM (2008) Genomic loss of microRNA-101 leads to overexpression of histone methyltransferase EZH2 in cancer. *Science* **322:** 1695–1699

Varambally S, Dhanasekaran SM, Zhou M, Barrette TR, Kumar-Sinha C, Sanda MG, Ghosh D, Pienta KJ, Sewalt RG, Otte AP, Rubin MA, Chinnaiyan AM (2002) The polycomb group protein EZH2 is involved in progression of prostate cancer. *Nature* **419:** 624–629

Vassilopoulos A, Wang RH, Petrovas C, Ambrozak D, Koup R, Deng CX (2008) Identification and characterization of cancer initiating cells from BRCA1 related mammary tumors using markers for normal mammary stem cells. *Int J Biol Sci* **4:** 133–142

Vissers JH, van Lohuizen M, Citterio E (2012) The emerging role of Polycomb repressors in the response to DNA damage. *J Cell Sci* **125:** 3939–3948

Wei Y, Chen YH, Li LY, Lang J, Yeh SP, Shi B, Yang CC, Yang JY, Lin CY, Lai CC, Hung MC (2011) CDK1-dependent phosphorylation of EZH2 suppresses methylation of H3K27 and promotes osteogenic differentiation of human mesenchymal stem cells. *Nat Cell Biol* **13:** 87–94

Wooster R, Weber BL (2003) Breast and ovarian cancer. *N Engl J Med* **348:** 2339–2347

Wu SC, Zhang Y (2011) Cyclin-dependent kinase 1 (CDK1)-mediated phosphorylation of enhancer of zeste 2 (Ezh2) regulates its stability. *J Biol Chem* **286:** 28511–28519

Xie D, Gore C, Liu J, Pong RC, Mason R, Hao G, Long M, Kabbani W, Yu L, Zhang H, Chen H, Sun X, Boothman DA, Min W, Hsieh JT (2010) Role of DAB2IP in modulating epithelial-to-mesenchymal transition and prostate cancer metastasis. *Proc Natl Acad Sci USA* **107:** 2485–2490

Xu K, Wu ZJ, Groner AC, He HH, Cai C, Lis RT, Wu X, Stack EC, Loda M, Liu T, Xu H, Cato L, Thornton JE, Gregory RI, Morrissey C, Vessella RL, Montironi R, Magi-Galluzzi C, Kantoff PW, Balk SP *et al* (2012) EZH2 oncogenic activity in castration-resistant prostate cancer cells is Polycomb-independent. *Science* **338:** 1465–1469

Yap KL, Li S, Munoz-Cabello AM, Raguz S, Zeng L, Mujtaba S, Gil J, Walsh MJ, Zhou MM (2010) Molecular interplay of the noncoding RNA ANRIL and methylated histone H3 lysine 27 by polycomb CBX7 in transcriptional silencing of INK4a. *Mol Cell* **38:** 662–674

Yu X, Chini CC, He M, Mer G, Chen J (2003) The BRCT domain is a phospho-protein binding domain. *Science* **302:** 639–642

Zhao J, Ohsumi TK, Kung JT, Ogawa Y, Grau DJ, Sarma K, Song JJ, Kingston RE, Borowsky M, Lee JT (2010) Genome-wide identification of polycomb-associated RNAs by RIP-seq. *Mol Cell* **40:** 939–953

Zhao J, Sun BK, Erwin JA, Song JJ, Lee JT (2008) Polycomb proteins targeted by a short repeat RNA to the mouse X chromosome. *Science* **322:** 750–756

Zhu Q, Pao GM, Huynh AM, Suh H, Tonnu N, Nederlof PM, Gage FH, Verma IM (2011) BRCA1 tumour suppression occurs via heterochromatin-mediated silencing. *Nature* **477:** 179–184